# Current Sensor Fault Detection and Isolation combining Model-Based and Signal-Based Algorithms in PMSG Drives

Yves Mollet*, Johan Gyselinck*, Fabien Meinguet+
*ECOLE POLYTECHNIQUE DE BRUXELLES, UNIVERSITE LIBRE DE BRUXELLES
Avenue Franklin Roosevelt 50 (CP165/52)
B-1050 Brussels, Belgium
Phone: +32 (0) 2 650 26 61
Fax: +32 (0) 2 650 26 53
Email: ymollet@ulb.ac.be
URL: http://beams.ulb.ac.be/energy/staff.html
+ARTS ET METIERS - PARISTECH
8 Bd Louis XIV - 59046 Lille, France

June 15th, 2013

## Keywords

<<Current sensor>>, <<Fault tolerance>>, <<Permanent magnet motor>>, <<Signal processing>>, <<Variable speed drive>>.

## Abstract

This paper presents a new on-line open-phase and current-sensor fault detection and isolation method for permanent-magnet synchronous generator (PMSG) drives with neutral point voltage control. Simple signal processing implementations for sensor outage and open-phase faults detection are combined with a cumulative-sum (CUSUM) algorithm capable of detecting smaller sensor output errors (offset or gain variation). The algorithm uses output signals from eight current sensors (two on each phase and two on the neutral wire). Experimental tests have been done on a 2kW-PMSG at different speeds and braking torques where different sensor-fault combinations have been tested with and without open-phase fault. Finally a test has been done while the shaft speed and the torque were varying in order to test the ability of the algorithm to work in transient conditions. Results show that the algorithm allows 3-out-of-6 redundancy in case of sensor outage and 5-out-of-6 redundancy in case of sensor offset or gain change with globally limited computational cost. Combinations of two outages and one offset or gain error can be isolated. In case of open-phase fault the algorithm can continue to detect sensor faults if at least one sensor is working on each remaining phase and on the neutral. A short fault detection time is obtained in case of sensor outage with a transitional detection by the CUSUM algorithm followed by the final detection by the signal processing algorithm.

## Introduction

PMSGs are more and more attractive for offshore wind power applications, thanks to the possibility of direct-drive configuration and to the increasing performance of permanent magnets [1]. They also appear as a better alternative than doubly-fed induction generators in marine current turbine applications [2]. Their high power density and high efficiency make them very attractive for aerospace applications [3]. In such applications reliability is of paramount importance, because of hostile environment and difficult access. In some cases an unplanned stop can lead to catastrophic consequences.

Redundancy or conservative design (i.e. using redundant or over-sized equipment) can improve reliability, but at high costs. On the other side, system monitoring enables detecting faults in an early stage, reducing repair costs and allowing for a planned maintenance operation. Therefore diverse fault detection and isolation (FDI) techniques are proposed, in which physical faults in the machine or in the converter are detected, as well as sensor faults, that can jeopardize correct operation of the closed-loop monitoring system of the generator [4] and generate secondary faults [5].

Patton et al. [6] divide FDI techniques into three categories: model-based, knowledge-based and empirical methods. The first category of methods can use quantitative or qualitative models. In the first case models such as transfer functions or differential equations are used to define residuals that undergo changes in case of a fault. This method is used in [7] to detect sensor faults in a PMSM-drive by summing the phase and neutral currents. In [8] PLLs and a CUSUM (cumulative sum) decision algorithm are used to detect open-phase faults. Chung et al. [9] propose to correct sensor offset and sensitivity error by measuring the resulting torque oscillation frequency. Qualitative model-based methods compare real observations with predicted behavior of the system in normal and several faulty conditions. These methods are sensitive to system parameters and need high computational power [5].

Knowledge-based methods are based on other approaches such as fuzzy logic and neural networks. Therefore no explicit model is needed but the required tuning effort may be considerable.

The last category relies on signal processing such as spectral analysis. In [5] simple mathematical operations are done in real-time on the current sensor signals in order to detect open-phase faults and sensor outages.

Considering the pros and cons of the existent techniques this paper proposes a combination of signal processing and model-based observers for open-phase and current sensor FDI on a PMSG. The replacement of a part of the model-based algorithm by signal processing will reduce the global need of computational power, while comparison between the respective model outputs will enable distinguishing sensor total outage from smaller output errors. The algorithm is adapted to a four-wire machine connection, enabling neutral point voltage control in case of open-phase fault. Ground faults and converter open-switch faults are not considered in this paper.

# Fault detection schemes

Two detection approaches are combined in this paper: a model-based algorithm using residuals and CUSUM functions proposed in [7] and in [10] on the one hand, a signal-based technique developed in [5] on the other hand.

## Technique using residuals and CUSUM detection algorithm

The model-based algorithm relies on the computation of fault indexes called residuals and is described in [7] and [10]. The number of residuals $n_r$ must be sufficiently high in order to be able to isolate all possible faults.

Since the residuals can be influenced by more than one fault or can change with the operational conditions, the average values of residuals must be known for healthy operation and in each faulty case. The sensitive or insensitive character of each residual must be listed for all investigated faults in an incidence table (see Table I).

Table I: Example of incidence table. A 1 (0) means that the residual is (not) affected by the fault

| | Fault 1 | Fault 2 | ... | Fault $n_f$ |
|---|---|---|---|---|
| Residual 1 | 1 | 0 | ... | 1 |
| Residual 2 | 0 | 0 | ... | 1 |
| ... | ... | ... | ... | ... |
| Residual $n_r$ | 0 | 1 | ... | 0 |

When the system is healthy, the different residuals form a vector $\mathbf{r}(k)$ of $n_r$ Gaussian white-noise sequences characterized by the mean vector $\boldsymbol{\mu}_0$ and the variance matrix $\boldsymbol{\Sigma}$. In case a fault $i$ occurs, only the mean is assumed to take another value $\boldsymbol{\mu}_{0i}$ while the variance is supposed unaffected.

For each hypothetical faulty case the log-likelihood ratio (LLR) between the considered hypothesis and the no-fault hypothesis is computed for each sample $k$:

$$s_{i,0}(k) = \ln \frac{p_i(\mathbf{r}(k))}{p_0(\mathbf{r}(k))} \tag{1}$$

where $p_0(\mathbf{r})$ and $p_i(\mathbf{r})$ are the probability density functions of vector $\mathbf{r}$ under the hypothesis that no fault occurs and that fault $i$ occurs respectively.

For each possible fault $i$ the cumulative sum (CUSUM) $S_{i,0}$ of the LLR is taken:

 ISBN: 978-90-75815-17-7 and 978-1-4799-0114-2 

$$S_{i,0}(k) = \sum_{j=1}^{k} \ln \frac{p_i(\mathbf{r}(i))}{p_0(\mathbf{r}(i))} \tag{2}$$

The CUSUM, as written in the equation above, is a decreasing function if fault $i$ is absent and an increasing function if fault $i$ is present. The practical implementation of the CUSUM is done in a recursive form $g_{i,0}(k)$, which maintains the output at zero in case the fault $i$ is not present:

$$g_{i,0}(k) = \max\left(0, g_{i,0}(k-1) + s_{i,0}(k)\right) \tag{3}$$

Finally, the most probable hypothesis is determined by comparing the CUSUM functions with each other and with a threshold value, using the decision function defined as :

$$g^{\star}_{l,0}(k) = \min_{\substack{i \in \{1,\ldots,n_f\} \\ i \neq l}} \left(g_{l,0}(k) - g_{i,0}(k) - h_{l,i}\right) \tag{4}$$

with $l \in \left\{1,\ldots,n_f\right\}$, $g_{0,0} = 0$ and $h_{l,i}$ a threshold value. The fault is then flagged when $g^{\star}_{l,0}(k) > 0$.

The approach described in [7] uses the differences between phase-locked loop based current frequency measurements and encoder frequency measurement as residuals for open-phase fault detection. To detect current sensor faults (gain or offset change or outage) and ground faults, the computation of residuals needs two current sensors per phase (six in all). The residuals are, on the one hand, the output differences between sensors on the same phase and, on the other hand, all possible sums that combine three current measurements from different phases.

## Signal processing algorithm

This signal processing method is proposed in [5]. The maximum of the absolute values of the instantaneous phase currents is computed at each time step to normalize the currents:

$$i_{mN} = \frac{i_m}{\max\{|i_a|, |i_b|, |i_c|\}} \tag{5}$$

with $m \in \{a,b,c\}$ and $N$ for normalized quantity. Four indicators are used in order to locate the fault and to distinguish an open-phase fault from a current-sensor outage. The detection indicator $d$ is the average absolute value of the sum of the normalized instantaneous currents:

$$d = \langle \Big|\sum_m i_{mN}\Big| \rangle = \frac{\omega}{2\pi}\int_0^{2\pi/\omega} \Big|\sum_m i_{mN}\Big| \, dt \tag{6}$$

where $\langle X \rangle$ is the average of X over one period and $\omega$ the pulsation of the currents.

This value remains close to zero except in case of ground fault and of current-sensor outage.

The localization indicators $l_m$ use the average absolute values of the normalized currents $\langle |i_{mN}| \rangle$ as follows:

$$l_m = \xi - \langle |i_{mN}| \rangle = \xi - \frac{\omega}{2\pi}\int_0^{2\pi/\omega} |i_{mN}| \, dt \tag{7}$$

where $\xi = 2/3$ is the value taken by $\langle |i_{mN}| \rangle$ in no-fault condition and in case the currents are perfectly balanced.

When the phase is healthy, $l_m$ is equal to zero while in case of zero current or current-sensor outage this value goes to $\xi$. In case of an open-circuit fault that does not result in a null current in the phase (e.g. if one of the two switches of one leg of the inverter fails open) this average can take an intermediate value.

By comparing the indicators with thresholds the type and the location of the fault can be determined.

A last indicator ($\theta_m$) is implemented with a minimal increase of computation power to determine and correct the current sensor offsets before starting the machine:

$$\theta_m = sign(i_{mN}) \langle \max\{|i_a|, |i_b|, |i_c|\} \rangle \langle |i_{mN}| \rangle \tag{8}$$

This algorithm presented in [5] can consequently detect and locate an open-circuit fault or a current sensor fault only using three current measurements (see Figure 1). However, only total outages are considered for the detection of sensor faults.

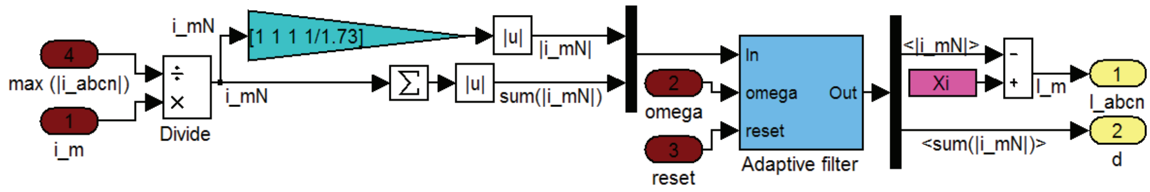


Figure 1: Simulink model of Freire's fault detection technique [5] (with minor changes). The neutral current is integrated in the current signal vector. All current are first normalized using the *Divide* block. An adaptive low-pass filter is used in order to get the average values of $|i_{m,N}|$ and of $|\sum_m i_{m,N}|$ for the computation of $l_m$ and $d$ respectively.

The presence of the $1/\sqrt{3}$ factor for the neutral current is needed since its amplitude is $\sqrt{3}$ higher than the ones of the remaining phase currents in open-phase post fault control.

## Proposed fault detection algorithm

The proposed algorithm combines the two previously explained techniques, using eight current sensors (two on each phase and two on the neutral wire of the PMSG). The algorithm is composed of two stages. The first one uses the signal processing algorithm in order to detect and isolate sensor outages. The second stage detects and isolates, on the one hand, open-circuit faults again with the signal processing algorithm, and on the other hand, sensor offsets or sensitivity errors using the CUSUM algorithm. The 4-wire connection is used together with a 4-leg inverter to keep the system working in case of one open-phase fault. In this case the neutral point potential is controlled by the supplementary leg of the converter in order to limit torque oscillations (see Figure 2).

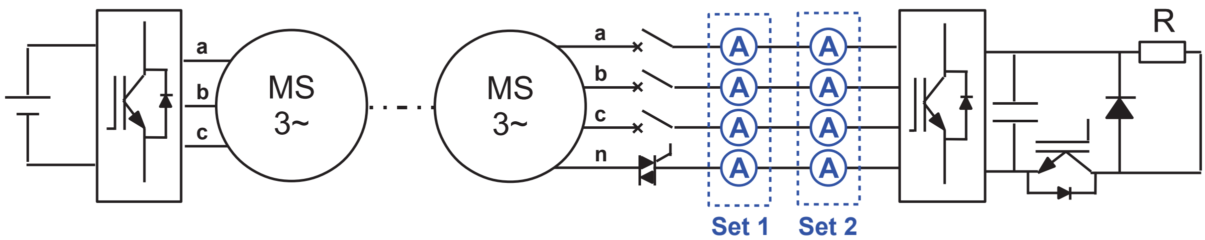


Figure 2: Test bench configuration with four-wire PMSG connection used for the experimental validation of the algorithm. The PMSG is driven at variable speed by a PMSM. The phases of the PMSG are connected to the converter through circuit breakers that are used to generate open-circuit-faults, while the triac is used by the controller to connect the neutral wire in case of open-phase fault. Two sets of four sensors are used to measure the currents in the phases and in the neutral wire of the PMSG.

In the first stage, the signal processing algorithm is implemented once for each group of four sensors to detect sensor outages. Some modifications are also done to the block diagram shown in Figure 1. Four signals (three phases and neutral) are processed instead of three in [5]. All eight sensor outputs are taken into account for the normalization (see equation 5) in order to make this operation less sensitive to sensor outages or to open-phase faults. Therefore the algorithm is able to continue to detect new faults, even if faults are already present. A saturation block is also added in the implementation of the normalization to avoid errors in case of zero current (or outage of all sensors). For this purpose the neutral current signals are multiplied by a factor $1/\sqrt{3}$, since their amplitudes are $\sqrt{3}$ times bigger than the ones of the currents flowing in the remaining healthy phases in case of open-phase post-fault control [7] while they remain null in case all phases are healthy.

The average values $\langle|\sum_m i_{mN}|\rangle$ and $\langle|i_{mN}|\rangle$ computed for the $d$ and $l_m$ indicators are approached using an adaptive low-pass filter with a cut-off pulsation equal to $\omega/\pi$, where $\omega$ is the current pulsation. The current sensor signals entering this stage are high-passed using an adaptive filter to remove their DC component. Therefore, the output falls necessarily to zero in case of sensor outage, which makes the detection easier. The cut-off pulsation of the high-pass filter is equal to $\omega/10$.

The processed signals are then compared to thresholds values in order to generate fault flags. For sensor outage detection both $d$ and corresponding $l_m$ indicators have to cross the threshold value. The flags are then used to control software switches in order to select the best suited current measurements for the PMSM control (see Figure 3). The current sensor signals used in this selection are not high-pass filtered, so that the second stage can work properly.

 ISBN: 978-90-75815-17-7 and 978-1-4799-0114-2 

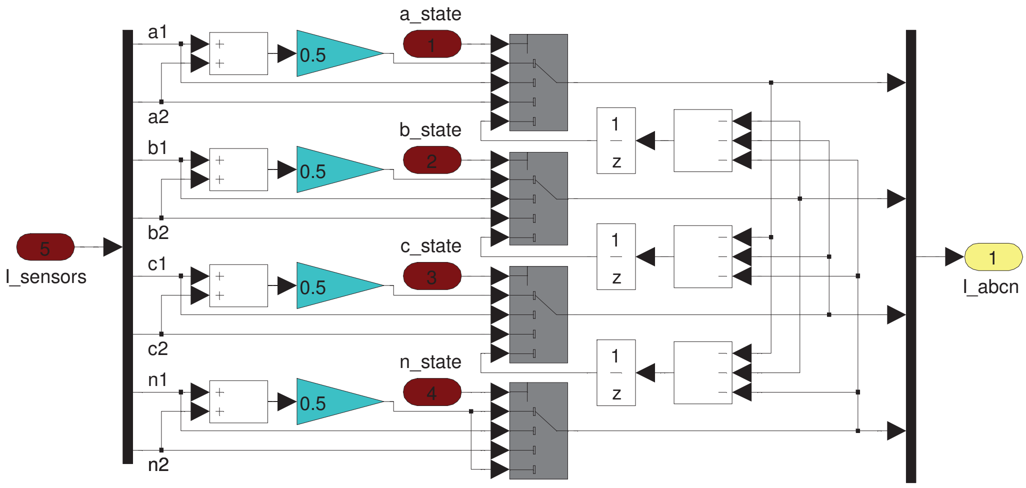


Figure 3: Simulink block for faulty sensor isolation. If both sensors of the phase are healthy, the average of both sensor outputs is chosen. If one of both sensors is faulty, the other sensor output is chosen. In the situation where both sensors of a phase are faulty, the phase current is computed by summing the opposite of the currents flowing in the other wires. In case both neutral current measurements are zero, however, the zero value is maintained, since this situation is normal in case no phase is open.

In the second stage of the algorithm the open-phase fault detection is achieved by a third implementation of the signal processing algorithm, made on the output of the current measurement selection block. In this way the open-phase detection is not affected by faulty sensors, as long as at least one sensor is working on each healthy phase and one on the neutral wire. An open-phase fault is flagged when the corresponding $l_m$ indicator crosses the threshold. In this case the corresponding sensor fault flags are inhibited, since the $l_m$ indicators in the first stage cross their threshold. Erroneous detection can then happen in case a $d$ indicator is above its threshold due to the outage of another sensor.

Moreover, a sensor gain or offset error detection is done using the CUSUM algorithm based on residuals computed from the sensor output signals. Since ground faults are not taken into account here, the residuals are limited to the signal differences between two sensors on each phase (and on the neutral) and to two sums of phase and neutral currents (see table II). The $g^{\star}$ indicators are defined using these residuals in the same way as explained in the section about the CUSUM algorithm. In case a sensor outage is already detected by the first stage, its signal is then replaced with the output of the current measurement selection block. This inhibits the corresponding flag and thus permits the CUSUM algorithm to detect one gain or offset error in addition to the sensor outages and open phases already detected.

Table II: Incidence table for the CUSUM-based part of the proposed algorithm. A 1 (0) means that the residual is (not) affected by the fault

| Residuals | $a1$ fault | $a2$ fault | $b1$ fault | $b2$ fault | $c1$ fault | $c2$ fault | $n1$ fault | $n2$ fault |
|---|---|---|---|---|---|---|---|---|
| $a1-a2$ | 1 | 1 | 0 | 0 | 0 | 0 | 0 | 0 |
| $b1-b2$ | 0 | 0 | 1 | 1 | 0 | 0 | 0 | 0 |
| $c1-c2$ | 0 | 0 | 0 | 0 | 1 | 1 | 0 | 0 |
| $n1-n2$ | 0 | 0 | 0 | 0 | 0 | 0 | 1 | 1 |
| $a1+b1+c1+n1$ | 1 | 0 | 1 | 0 | 1 | 0 | 1 | 0 |
| $a2+b2+c2+n2$ | 0 | 1 | 0 | 1 | 0 | 1 | 0 | 1 |

The algorithm combining model and signal processing enables 3-out-of-6 redundancy in case of sensor outage or 5-out-of-6 redundancy in case of sensor offset or gain error with a globally limited computational power. If a phase is open, the algorithm continues working with one faulty sensor (or two if they are on different phases) on the remaining phases or on the neutral.

## Experimental results

The PMSG used in the test bench is star-connected. The neutral point of the generator is also accessible and its potential can be controlled using a dedicated inverter (with four legs) using a dSPACE 1006

Table III: Main parameters of the PMSG

| Parameter | Symbol 2 | Value |
|---|---|---|
| Nominal voltage (phase-to-phase, RMS) | $V_{N,ph-ph}$ | 325 V |
| Nominal current (RMS) | $I_N$ | 5.7 A |
| Nominal power | $P_N$ | 2.59 kW |
| Nominal speed | $N_N$ | 2000 rpm |
| Stall torque (continuous) | $T_N$ | 13.5 Nm |

interface (see Figure 2). A braking chopper fixes the DC bus voltage to 225 V. The main characteristics of the machine are presented in Table III.

The fourth leg of the inverter is connected to the neutral wire through a triac as soon as an open-phase fault is detected and the control is modified in order to reduce as much as possible the torque oscillations. The implemented control reconfiguration method, coming from [7], is briefly explained below.

In order to suppress the ripple on the torque, the post-fault $dq$ components of the current must remain equal to the ones before the fault. This is done by imposing a zero-sequence current reference $I_0^\star$, which depends on the current references $Iq^\star$ and $I_q^\star$:

$$I_0^\star = \sqrt{2}\left(I_q^\star \sin\left(\theta_e - k\frac{2\pi}{3}\right) - I_d^\star \cos\left(\theta_e - k\frac{2\pi}{3}\right)\right) \tag{9}$$

with $\theta_e$ the electrical position of the rotor and $k = 0, 1, 2$ when phase $a$, $b$ or $c$ respectively open.
This current is imposed by means of a feed-forward action consisting in a change in the zero-sequence voltage reference $\Delta V_0^\star$ according to the stator resistance $R_s$ and to the stator homopolar inductance $L_0$ :

$$\Delta V_0^\star = R_s I_0 + L_0 \frac{dI_0^\star}{dt} \tag{10}$$

A complementary feed-back loop on the $I_0$ current is also implemented. The resulting healthy phase currents increase by a factor $\sqrt{3}$ and the neutral current reaches three times the current that was flowing in the phases before the fault.

Measurement redundancy is obtained by using double current measurements on each phase and on the neutral wire. The sensor outputs are denoted by subscripts $a1$, $a2$, $b1$, $b2$, $c1$, $c2$, $n1$ and $n2$. Their rating (17.5 A = 1 pu) is used as basis for the quantification of the faults.

A 2kW-PMSM coupled to the investigated generator is used as a motor and is driven using vector control (with another dSPACE interface or with a commercial drive) in order to impose the rotational speed. The control of the generator is indeed used to fix the braking torque.

In order to validate the combined algorithm, tests are done for different fault cases at different torques and rotational speeds. For all cases the defined thresholds for $l_m$ and $d$ are 0.15 for sensor faults detection, and the threshold for $l_m$ is fixed to 0.3 for open-phase detection. The threshold for the indicators generated by the CUSUM algorithm is fixed to 0.08.

## Current sensor faults

The response of the algorithm to a combination of sensor faults is presented in Figure 4.

The PMSG is driven at 200 rpm and its braking torque is 10 Nm. Sensors $c2$ and $b2$ outputs are disconnected at 4.493 s and 4.630 s respectively. An offset of 0.7 A (0.08 pu referring to the sensor nominal current) is added to the output of sensor $a1$ at 4.822 s. The sensor outages are first detected by the CUSUM algorithm (each after 0.002 s). The detection with the signal processing algorithm happens at 4.533 s and 4.676 s respectively (0.040 s and 0.036 s after the fault), when the respective $l_m$ and $d$ indicators have both crossed their threshold. As soon as the sensor outage is detected by the signal processing algorithm, the corresponding CUSUM indicator is inhibited and the corresponding indicator goes back to zero. According to the evolution of the corresponding output of the CUSUM algorithm the offset error is detected after 0.005 s. Because the signal is higher than normal this fault is not seen by the signal processing algorithm.


ISBN: 978-90-75815-17-7 and 978-1-4799-0114-2

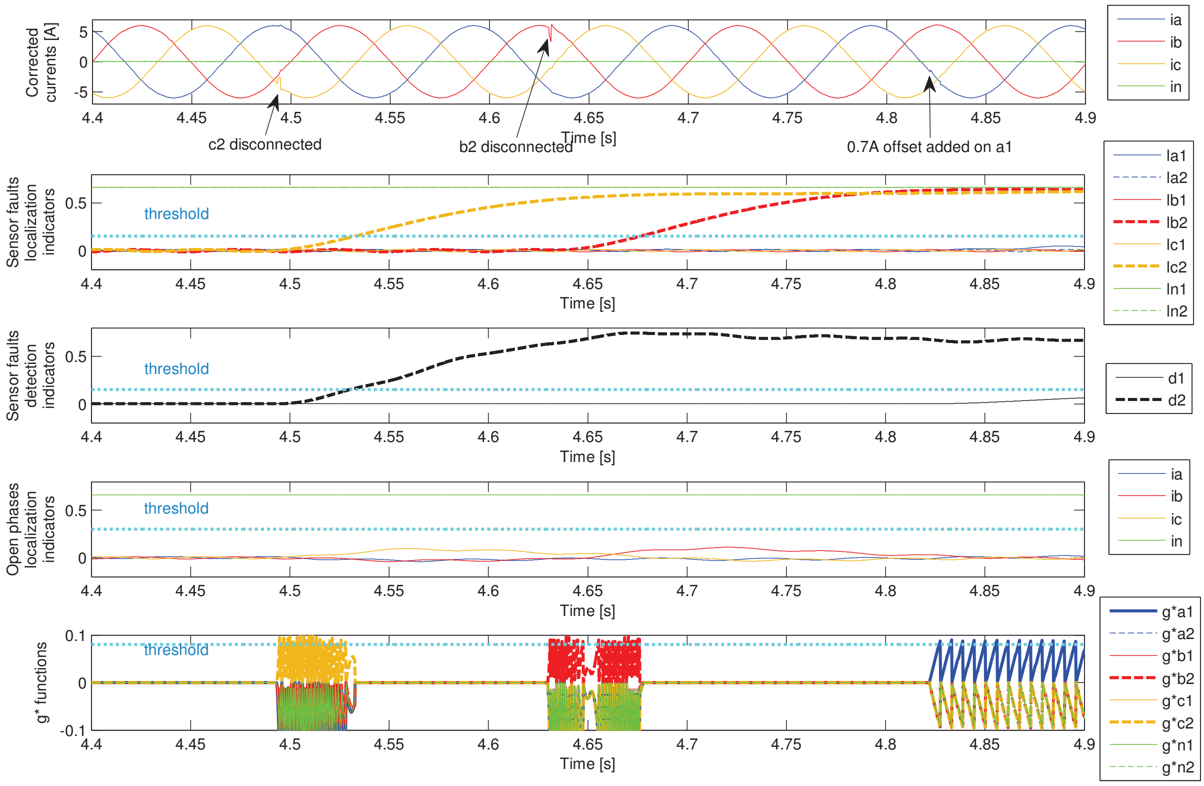


Figure 4: Detection of two sensor outages followed by a current sensor offset error on the PMSG running at 200 rpm with a 10 Nm-braking torque. Sensors $c2$ and $b2$ are disconnected at 4.493 s and 4.630 s respectively and an offset is added to sensor $a1$ output at 4.822 s. From top to bottom: current measurements at the output of the selection block, sensor faults related $l_m$ and $d$ indicators, open-phase fault related $l_m$ indicators and $g^\star$ indicators for sensor gain or offset error detection.

## Current sensor faults combined with an open phase

The response of the algorithm to situations combining an open-phase fault and sensor faults are presented in Figures 5 and 6.

In Figure 5 the PMSG is driven at 800 rpm and its braking torque is 10 Nm. The gain of sensor $a2$ is multiplied by 1.09 (corresponding to a peak difference of 0.7 A) at 3.471 s. Sensor $c2$ output is disconnected and phase b is opened at 3.848 s and 4.297 s respectively. According to the evolution of the corresponding output of the CUSUM algorithm the sensor gain fault is detected after 0.006 s. Because the signal is higher than normal this fault is not seen by the signal processing algorithm. The sensor outage is first detected by the CUSUM algorithm (after 0.002 s). The detection with the signal processing algorithm happens at 3.857 s (0.009 s after the fault). Since the CUSUM algorithm only detects the most deviating sensor, the gain error of sensor $a2$ is temporary no more detected. This introduces an error in the current values that are used for the control of the machine, but this error is reduced compared to the case $c2$ is not compensated. As soon as the sensor outage is detected by the signal processing algorithm, the corresponding CUSUM indicator is inhibited and the error on $a2$ sensor output is again taken into account. The open-phase fault is finally detected at 4.315 s (0.018 s after the fault); the neutral voltage starts then to be controlled as it can be seen from the apparition of a neutral current. It can be noted that the indicators $l_{b1}$ and $l_{b2}$ cross their own threshold at 4.309 s. Due to the fact that the indicator $d_2$ has already crossed its threshold because of the outage of sensor $c2$, a erroneous outage is detected for sensor $b2$. This has however no influence on the corrected currents, since sensor $b1$ output is then selected and remains correct. With the open-phase detection the sensor fault is inhibited and the problem disappears. The same phenomenon also happens with sensor $n2$ in the interval in which indicator $l_n$ has already crossed its threshold and indicators $l_{n1}$ while $l_{n2}$ are still above their one (i.e. at time between 4.333 s and 4.343 s).

In Figure 6 the PMSG is driven at 200 rpm and its braking torque is 2 Nm. At 2.604 s a 0.7 A offset is added to sensor $c2$ output. Sensor $b2$ is disconnected at 3.519 s and phase a is opened at 3.901 s. The offset on sensor $c2$ is detected by the CUSUM algorithm after 0.005 s. Sensor $b2$ outage is detected, once again, first by the CUSUM algorithm (after 0.012 s) and then by the signal processing algorithm (after 0.051 s). The open-phase fault is detected after 0.070 s. The erroneous sensor outage detection on sensors $a2$ and $n2$ again appear, but do not affect the control, as explained in the previous example.

By comparing the detection time for each algorithm for the different tests the principal influencing pa-


ISBN: 978-90-75815-17-7 and 978-1-4799-0114-2

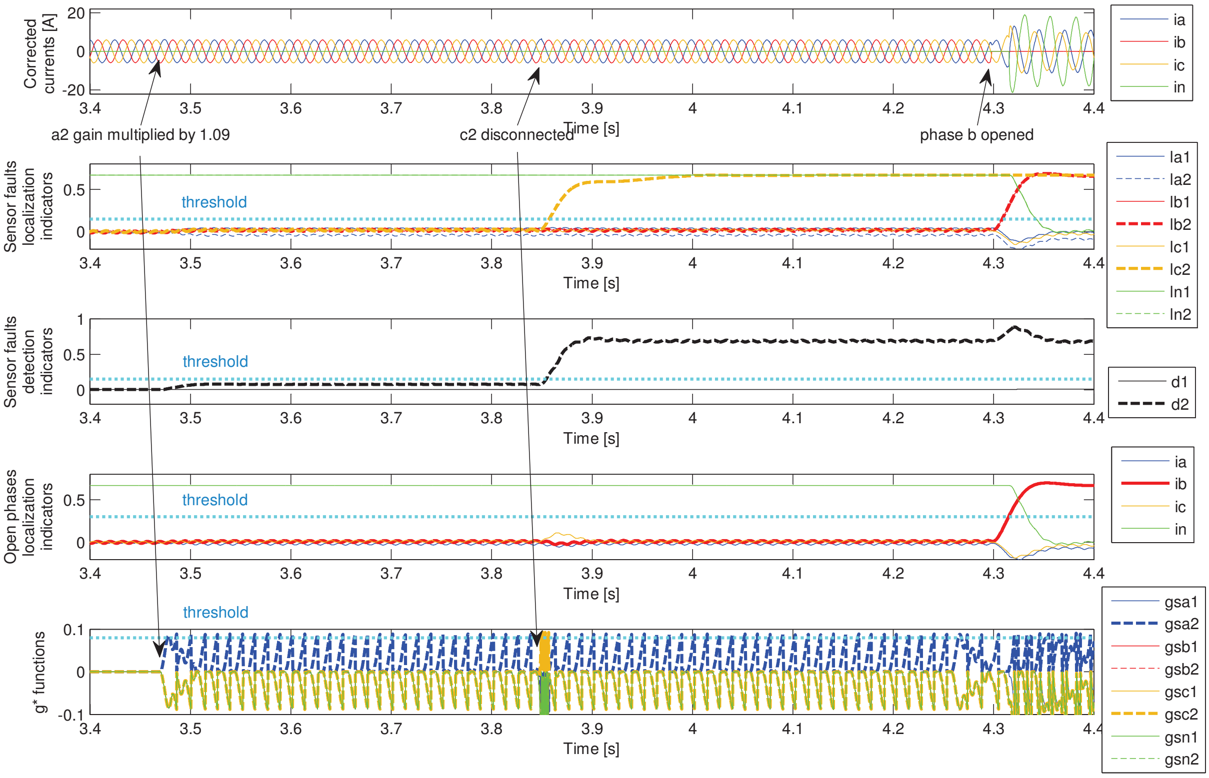


Figure 5: Detection of a current sensor gain error successively followed by a sensor outage and by an open-phase fault on the PMSG running at 800 rpm with a 10 Nm-braking torque. Sensor $a2$ gain is modified at 3.471 s; sensor $c2$ and phase b are respectively disconnected at 3.848 s and 4.297 s. From top to bottom: current measurements at the output of the selection block, sensor faults related $l_m$ and $d$ indicators, open-phase fault related $l_m$ indicators and $g^{\star}$ indicators for sensor gain or offset error detection.

rameters can be discussed. It turns out that the CUSUM algorithm seems not to be influenced by the frequency of the currents. On the contrary, the cut-off frequency of the adaptive filter used for the signal processing algorithm (see Figure 1) must be reduced in case of low speed, leading to slower detection dynamics. In addition, a smaller braking torque generates also smaller currents, and therefore the residuals of the CUSUM algorithm are reduced, increasing the detection time. This phenomenon is limited by the normalization in the case of the signal processing algorithm. It can be furthermore mentioned that the detection time is also affected by faults that are previously detected due to the fact that they can have an influence on indicators corresponding to other faults.

### Current sensor faults in transient state

In order to test the response of the algorithm in case of transient speed and torque a test has been done by forcing $c1$ sensor output to zero just after a change in the braking torque reference. The change of reference consists of a step from 2 to 6 Nm at 1.883 s. This torque step induces a temporary speed drop, before the speed controller of the driving motor reacts. The minimum speed (282 rpm) is reached at 2.002 s. The evolution of the shaft torque and speed is shown in Figure 7. The $c1$ sensor output is forced to zero at 1.896 s. The evolution of the currents and of the indicators is shown in Figure 8.

These results show that the amplitude and frequency change in the currents do not affect significantly the indicators. The only visible changes are generated by the sensor fault: the CUSUM algorithm detects and isolates the fault (after 0.002 s) followed by the signal processing algorithm (0.011 s after the fault).

## Conclusions

A new fault detection and isolation algorithm for PMSGs combining the advantages of model-based and signal processing techniques is proposed. The technique uses the output of eight current sensors (two on each phase and on the neutral wire of the PMSG).

The new combined algorithm permits 3-out-of-6 redundancy in case of sensor outage and 5-out-of-6 redundancy in case of sensor offset or gain error with a globally limited computational power. It can also

 ISBN: 978-90-75815-17-7 and 978-1-4799-0114-2 

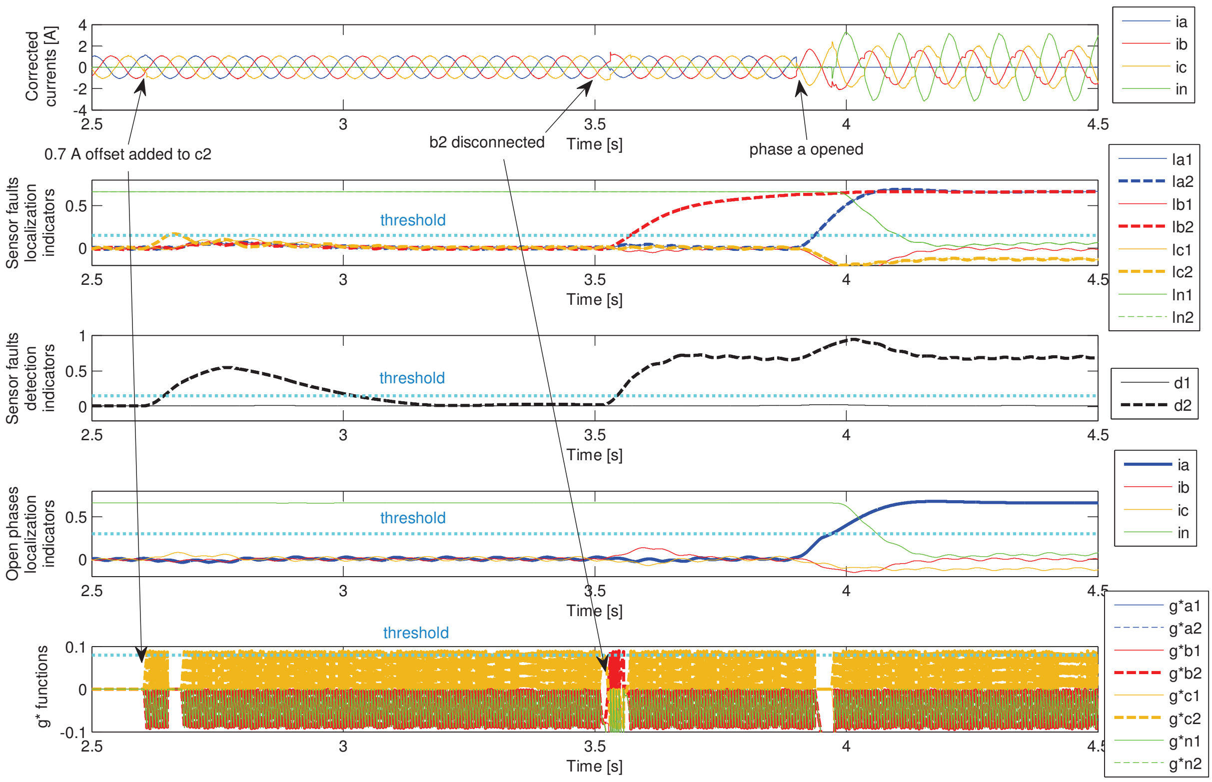


Figure 6: Detection of a current sensor offset error successively followed by a sensor outage and an open-phase fault on the PMSG running at 200 rpm with a 2 Nm-braking torque. An offset of 0.7 A is added to the output signal of sensor $c2$ at 2.604 s. Sensor $b2$ and phase a are disconnected at 3.519 s and 3.901 s respectively. From top to bottom: current measurements at the output of the selection block, sensor faults related $l_m$ and $d$ indicators, open-phase fault related $l_m$ indicators and $g^\star$ indicators for sensor gain or offset error detection.

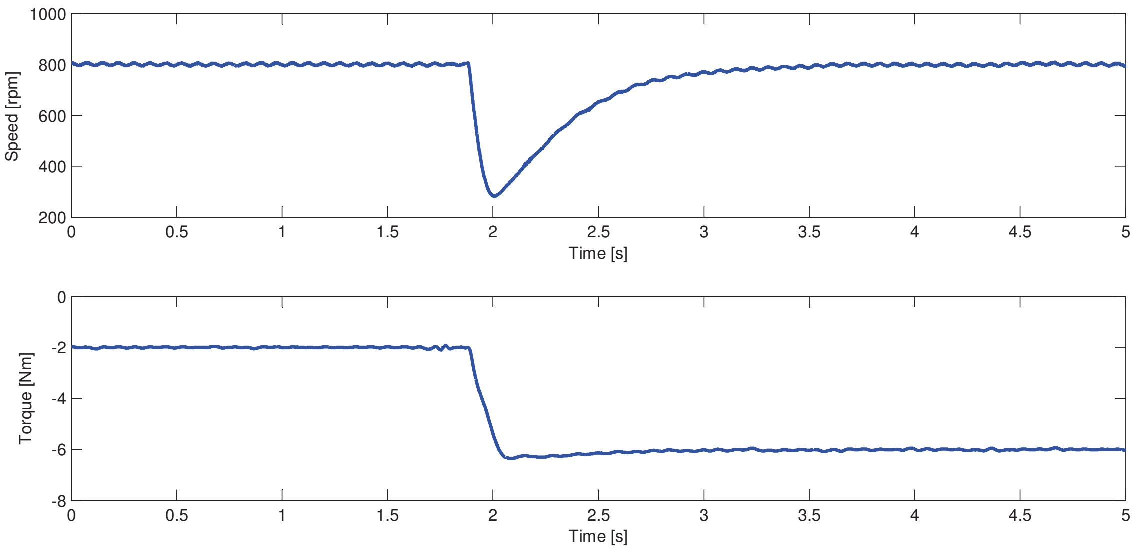


Figure 7: Evolution of the measured shaft torque (in Nm) and speed (in rpm) during the FDI test in transient state. The negative sign of the torque comes from the fact that the machine is in generator mode.

manage a combination of two outages and one offset or gain error. In case of open-phase fault it remains working if at least one sensor is working on each remaining phase and on the neutral.

The combination of CUSUM and signal processing also permits having a different diagnosis for sensor outage (detected by signal processing) and for sensor gain or offset errors (only detected by residuals generation and CUSUM detection system). In case of sensor outage the early detection by the CUSUM algorithm reduces the disturbance caused by the fault before its isolation.

 ISBN: 978-90-75815-17-7 and 978-1-4799-0114-2 

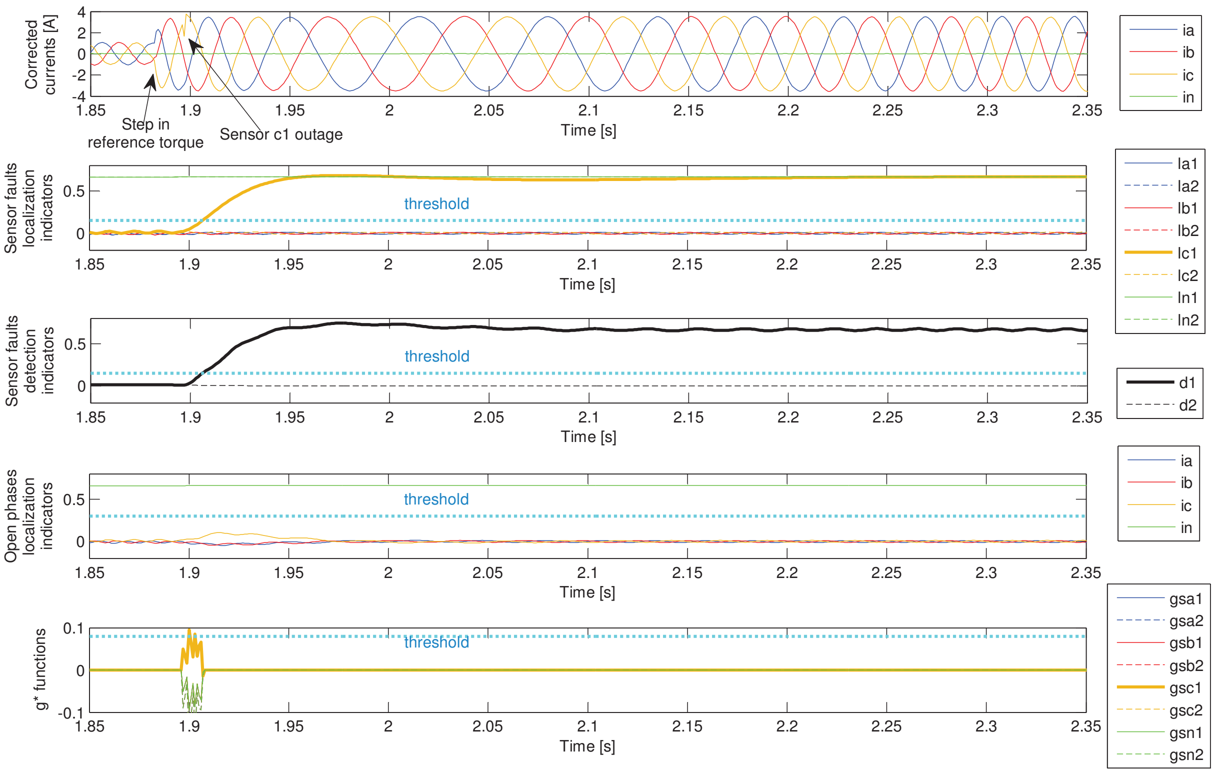


Figure 8: Detection of a current-sensor outage in transient state. At 1.883 s the reference braking torque is changed from 2 to 6 Nm, causing a speed transient with a minimum value of 282 rpm at 2.002 s. Sensor $c1$ output is set to zero at 1.896 s. From top to bottom: current measurements at the output of the selection block, sensor faults related $l_m$ and $d$ indicators, open-phase fault related $l_m$ indicators and sensor gain or offset error related $g^{\star}$ indicators.

The combined algorithm is not significantly affected by speed and torque transients. A fault can then be detected and isolated without false alarms in transient regimes.

# References


[1] Li H.; Chen Z. Overview of different wind generator systems and their comparisons. IET Renewable Power Generation, 2(2):123 - 138, 2008.

[2] Ng K.-W.; Lam W.-H.; and Ng K.-C. 2002-2012: 10 Years of Research Progress in Horizontal-Axis Marine Current Turbines, Energies, 6, 1497-1526, March 2013.

[3] Atkinson G.J.; Bennett J.W.; Mecrow B.C.; Atkinson D.J.; Jack A.G.; Pickert V. Fault tolerant drives for aerospace applications Integrated Power Electronics Systems (CIPS), 2010 6th International Conference on, paper 6.3, March 2010.

[4] Rothenhagen K. Current sensor fault detection, isolation, and reconfiguration for doubly fed induction generators. IEEE Transactions on industrial electronics, 56(10):4239 - 4245, October 2009.

[5] Freire N. M. A.; Estima J. O.; Cardoso A. J. M. A new approach for current sensor fault diagnosis in PMSG drives for wind energy conversion systems. In Energy Conversion Congress and Exposition (ECCE), 2012 IEEE, pages 2083 - 2090, September 2012.

[6] Patton R.; Frank P.; and Clark R. Issues of Fault Diagnosis for Dynamic Systems. , Berlin, Germany, 2000.

[7] Meinguet F. Fault-tolerant permanent-magnet synchronous machine drives - Fault detection and isolation, control reconfiguration and design considerations. PhD thesis, Université Libre de Bruxelles, 2012. Available: http://theses.ulb.ac.be/ETD-db/collection/available/ULBetd-12312011- 163524/unrestricted/phd Meinguet final.pdf.

[8] Meinguet F.; Kestelyn X.; Semail E. and Gyselinck J. Fault detection, isolation and control reconfiguration of three-phase pmsm drives. In Industrial Electronics (ISIE), 2011 IEEE International Symposium on, pages 2091 - 2096, June 2011.

[9] Chung D.-W.; Sul S.-K.; Lee D.-C. Analysis and compensation of current measurement error in vector-controlled ac motor drives. IEEE Transactions on Industry Applications, pages 388 - 393, 1998.

[10] Blanke M.; Kinnaert M.; Lunze J.; Staroswiecki M. Diagnosis and Fault-Tolerant Control. , 2 edition, 2006.